

Article

Enhancement in Nanomechanical, Thermal, and Abrasion Properties of SiO₂ Nanoparticle-Modified Epoxy Coatings

Mohammad Asif Alam ^{1,*}, Ubair Abdus Samad ¹, Manawwer Alam ^{2,*}, Arfat Anis ³  and Saeed M. Al-Zahrani ³

¹ Center of Excellence for Research in Engineering Materials (CEREM), King Saud University, P.O. Box 800, Riyadh 11421, Saudi Arabia; uabdussamad@ksu.edu.sa

² Department of Chemistry, College of Science, King Saud University, P.O. Box 2455, Riyadh 11451, Saudi Arabia

³ SABIC Polymer Research Center (SPRC), Chemical Engineering Department, King Saud University, P.O. Box 800, Riyadh 11421, Saudi Arabia; aarfat@ksu.edu.sa (A.A.); szahrani@ksu.edu.sa (S.M.A.-Z.)

* Correspondence: moalam@ksu.edu.sa (M.A.A.); maalam@ksu.edu.sa (M.A.)

Received: 27 February 2020; Accepted: 20 March 2020; Published: 25 March 2020



Abstract: Epoxy formulations containing 1%, 3%, and 5% SiO₂ nanoparticles (SNPs) were produced and applied to mild steel substrates in order to improve their thermal, nanomechanical, and abrasion resistance. Field emission scanning electron microscopy (FE-SEM) was used to analyze the dispersion of nanoparticles in the final coating samples, and Energy-dispersive X-ray spectroscopy (EDX) was used to confirm the presence of nanoparticles. Thermogravimetric analysis (TGA) was employed to measure the thermal resistance of the prepared coatings. Conventional techniques were used to measure the impact and scratch resistance. For nanomechanical testing, nanoindentation was performed using a Berkovich-type indenter. Using a taber abraser, the abrasion properties of the coatings were measured. The FE-SEM images indicated good dispersion of the nanoparticles at all three different loading levels. The scratch, impact, and hardness of coatings improved with the addition of the SNPs. Nanomechanical properties, such as hardness and elastic modulus, improved when compared to the unmodified coatings. The thermal and abrasion resistances of the coatings improved with the increase in the SNPs content of the coatings. The highest mechanical, thermal, and abrasion properties were obtained for the coatings with 5% SNP content.

Keywords: epoxy; silica; nanoparticles; abrasion; nanoindentation

1. Introduction

The application of organic and inorganic coatings has been well studied with respect to the protection of metals against corrosion and their effectiveness for various structures. However, despite the significant development in coating technologies, challenges remain in the long-term protection of metals from damage and aggressive environments. One of the main reasons for the limited number of high-performance coating systems is the complexity of coating substrate systems and the number of factors that affect the performance and service life of such protective coatings. In addition to the composition of the coating—which consists of resin, solvents, fillers, and additives, such as UV stabilizers and wetting agents—the performance and durability of the coatings depends on several other parameters, such as the type of substrate, pretreatment of the substrate, curing thickness of the coating, and adhesion between the substrate and the coating. For example, a high-performance protective and durable coating must have adequate flexibility and toughness while withstanding impact and cracking as well as maintaining its qualities when subjected to stress, mechanical damage,

and weathering. Recent efforts aimed at reducing the emissions of volatile organic compounds have motivated the coating-technology research community to develop products with high solid content, powder coatings, or water-borne coatings with fewer organic solvents. However, solvent-based coatings cannot be replaced with environmentally friendly coatings, owing to the high-performance requirements of various substrates. It is essential to study the interaction of the components of the coating compositions to develop formulations for high-performance applications [1]. Efforts are being made to explore such a material to fulfill all the shortcomings of the current protective coating systems to overcome various problems for protective coatings. Many studies that are related to coating systems containing nanoparticles have already been published, such as those on epoxy/TiO₂ and Latex/silica [2,3]. These investigations show that, when compared to conventional organic coatings containing micro fillers, the use of nanofillers has advantages, such as improvements in scratch, abrasion, heat, radiation, and swelling resistance; a decrease in water permeability; and, an increase in hardness, weatherability, and elastic modulus [4]. It becomes necessary to disperse the filler in the binder resin to obtain the desired results and properties to achieve a successful nanoparticles-incorporated coating.

Previously studies have already been conducted to develop a protective epoxy coating system for the marine environment, and there is sufficient interest in replacing inorganic anticorrosive additives with environmentally friendly additives. Shi et al. [5] used four different types of particles to incorporate in the epoxy matrix, including SiO₂, to check their effects on morphological, mechanical, and anticorrosive properties. They concluded that the presence of silica nanoparticles (SNPs) was the most effective way of enhancing the mechanical strength of coatings, and it was the second most effective in terms of the improvement of anticorrosive properties. Conradi et al. [6] applied a modified SNP coating on DSS 2205 type duplex stainless steel. He reported a significant 30% enhancement of hardness and a 4% increase in the fracture toughness in comparison to the pure epoxy sample. Palraj et al. [7] prepared epoxy coatings by synthesizing nanosilica while using the sol-gel process and compared the properties with those of microsilica. They reported an improvement in the mechanical properties (wear and impact resistance) of nanosilica-based coatings as compared with their microsilica-based equivalents. Nikje et al. [8] prepared SiO₂-reinforced epoxy composite coatings using in-situ polymerization, whereby the silica particles were treated prior to incorporation into the matrix resin. Their results concluded that, in comparison to unmodified coatings, there was an increase in both the thermal and mechanical properties of the modified coating.

The quality of the interface of the filler particle with the matrix and adhesion strength of the interface governs the load transfer from the matrix to the nanofillers thereby leading to improved mechanical properties [9]. Well dispersed nanoparticles are able to improve various properties of the nanocomposites at loading of 5% or less, which makes them an attractive system when compared to other composites systems [10,11]. Several studies have been conducted to elucidate the effect of the nanofiller content on the mechanical properties of polymer nanocomposites [12–19]. Epoxy reinforced with nanosilica was one of the most studied composite systems. Better improvements in mechanical properties were reported for smaller sized nanosilica fillers. Islam et. al. [20] reported the effect of the addition of 5% silica nanoparticles of 20 nm and found an improvement in the tensile stress, yield stress, and Young's modulus for the epoxy nanocomposites. A 20% increase in the ultimate stress and 50% increase in yield stress were observed for these 5% nanosilica reinforced epoxy composites. Zhang et al. [21] showed a reduction of 80% and 76% in the coefficient of friction and wear rate, respectively, for the coatings at room temperature by the incorporation of 4.0 wt.% graphene as compared to that of the neat epoxy coatings. Luo et al. [22] reported that basalt flake modified epoxy coatings that were incorporated with 3% nanosilica showed excellent chemical and mechanical performance. Yuan et al. [23] reported that the incorporation of titanium nanoparticle modified graphene oxide significantly improved the corrosion and wear resistance of the epoxy coatings.

Several of the above highlighted works used special techniques, such as in-situ polymerization and the sol-gel method. The authors in this work prepared SNP-modified coatings using a direct incorporation method, in which, after treating the SNPs, their dispersed phase was directly incorporated

and well dispersed into the epoxy matrix. Mixing was carried out using a mechanical mixer and ultrasonication. The mechanical, thermal, and abrasion properties of these SNP modified coatings are reported herein, whereas the electrochemical properties have already been studied and reported earlier [24].

2. Materials and Methods

Diglycidyl ether bisphenol-A (DGEBA; Hexion, Iserlohn, Germany) was the main formulating ingredient as a resin matrix, along with polyamidoamine adduct (Aradur D-450 BD; Huntsman Advance Materials, Germany), which was used as a hardener/crosslinker. Xylene and MIBK were used as solvents to prepare formulations to facilitate mixing and viscosity adjustments. The SNPs used in this study were purchased from Sigma–Aldrich (catalog number: 637238, St. Louis, MO, USA) having a particle size of 10–20 nm.

Three formulations with different percentages of SNPs (1%, 3%, and 5%) were prepared while using stoichiometric balanced amounts of epoxy resin and hardener. Initially, the resin was placed in a beaker and diluted using xylene as a solvent to facilitate mixing by means of a mechanical stirrer (Sheen S2 disperse master, Sheen instruments, Surrey, UK). SNPs, in contrast, were dispersed in acetone in the presence of silane while using the sonication technique to promote mixing in the resin. The nanoparticle mixture was subjected to sonication for 30 min. The dispersed nanoparticle solution was then added slowly to the diluted epoxy resin with continuous stirring using a mechanical stirrer at 500 RPM. After the addition of the dispersed nanoparticles, the formulation was subjected to mechanical mixing at high RPM (5000 RPM) for 45 min. to facilitate the dispersion and removal of the excess solvent. After complete mixing, the stoichiometric amount of hardener was added to complete the formulation. Table 1, below, shows the complete formulation ingredients and the quantities used to prepare the formulations.

Table 1. Formulation of epoxy/SiO₂ nanoparticle incorporated coatings.

Sample	* Resin	Xylene (mL)	MIBK (mL)	SiO ₂ (wt.%)	Air Release	Silane	* Hardener
Epoxy	83.34	10	10	0	1	2	16.66
SN-1	83.34	10	10	1	1	2	16.66
SN-3	83.34	10	10	3	1	2	16.66
SN-5	83.34	10	10	5	1	2	16.66

* Epoxy resin and hardener are balanced according to stoichiometry not according to wt.%.

The FE-SEM (Field emission scanning electron microscope, JEOL, Tokyo, Japan) model JSM-7400F was used to check the morphology of the coating samples along with Energy-dispersive X-ray spectroscopy (EDX) to check the distribution of the added nanoparticles in the final coatings. The samples were mounted to stubs using carbon tape and were then platinum-coated via sputtering.

Thermogravimetric analysis (TGA) was performed on the prepared coatings using a Q600 by TA instruments (New Castle, DE, USA) to observe the thermal stability and decomposition temperatures. A standard aluminum pan was used for this purpose and the samples were heated from room temperature (25 °C) to 600 °C under a N₂ environment with a ramping rate of 10 °C/min.

The surface hardness of the coatings was measured using a Koenig pendulum tester (model 707/K) by Sheen Instruments, Surrey, UK, following the ASTM D-4366, where a higher number of oscillations defines a higher surface hardness. A scratch tester (model 705, Sheen Instruments, Surrey, UK) following the ASTM D-7027 was used in order to measure the scratch resistance of the prepared coatings. The maximum load (in kg) that is sustained by the coatings determines the coatings' scratch resistance. To check the impact resistance of the coatings, a BYK-Gardener impact tester was used (model IG-1120, BYK, Columbia, USA) following the ASTM D-2794 while using a standard weight of 8 lb. The results for pendulum hardness, scratch, and impact resistance are provided as average of the results of the three test specimens.

Using the Nanotest platform from micromaterials, UK, nanomechanical properties, such as the elastic modulus and the hardness of the prepared coatings were determined using a Berkovich-type indenter (Micromaterials, Wrexham, UK). A load control program was used to determine the coating properties by subjecting them to a maximum load of 100 mN. The samples were indented at $1 \text{ mN}\cdot\text{s}^{-1}$ until a predetermined load of 100 mN was achieved, followed by a holding period of 60 s. Finally unloading was started at the same strain rate of $1 \text{ mN}\cdot\text{s}^{-1}$ until the complete removal of the load. The results obtained through indentation were analyzed using software that was provided with the machine. To obtain result uniformity, at least 10 indentations were performed, although the final obtained results were averaged.

A taber abrader with a dual rotary platform (model 5155) was used using CS-17 wheels (Sheen Instruments, Surrey, UK) to measure the abrasion resistance of the coated samples. Initially, the samples were subjected to abrasion for 500 cycles at a speed of 60 cycles per minute. After 500 cycles, the abrading wheels were refaced for 50 cycles; subsequently, another 500 cycles of abrasion were performed, amounting to a total of 1000 cycles on each sample. Finally, the weight loss was calculated after 1000 cycles by subtracting the final weight from the initial weight. Three samples were tested and the average value was reported for each formulation.

3. Results and Discussion

3.1. Field Emission Scanning Electron Microscopy (FE-SEM)

Figure 1A–D show the FE-SEM images for unmodified and SNP-modified coatings; all of the images were taken at the same magnification. Figure 1A shows a smooth and plain surface of the epoxy material without the presence of any particles. With the addition of nanoparticles in the epoxy, starting from 1%, followed by 3%, and 5%, changes can be seen from Figure 1B–D. The images show that the nanoparticles are well dispersed and distributed throughout the matrix, with quite a few aggregate formations. The formation of aggregates with the use of nanoparticles is common, happening because of the high attraction forces between nanoparticles due to their high surface area. Another reason is the mixing of particles in a high viscous matrix [25]. EDX was simultaneously performed with SEM; Table 2 shows the overall composition of elements obtained in the EDX.

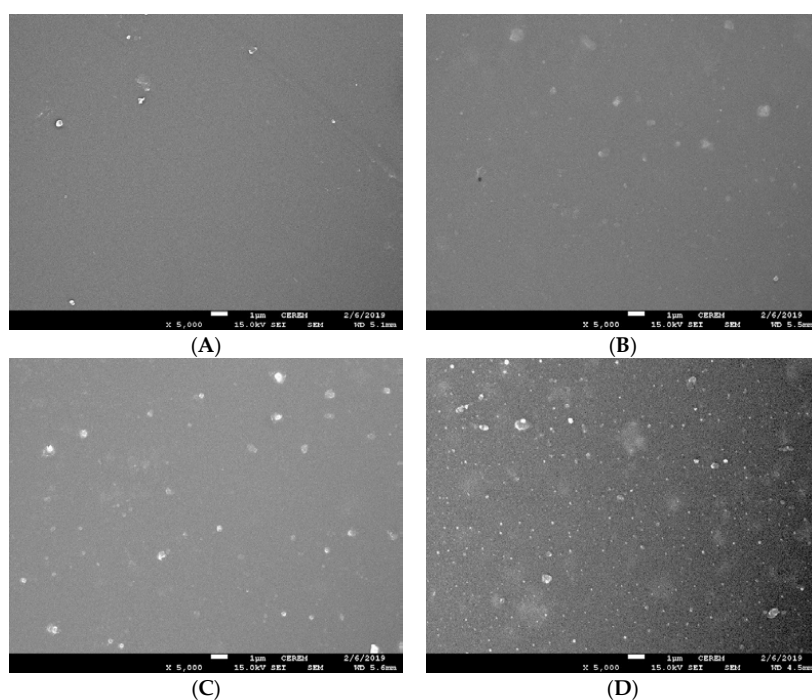


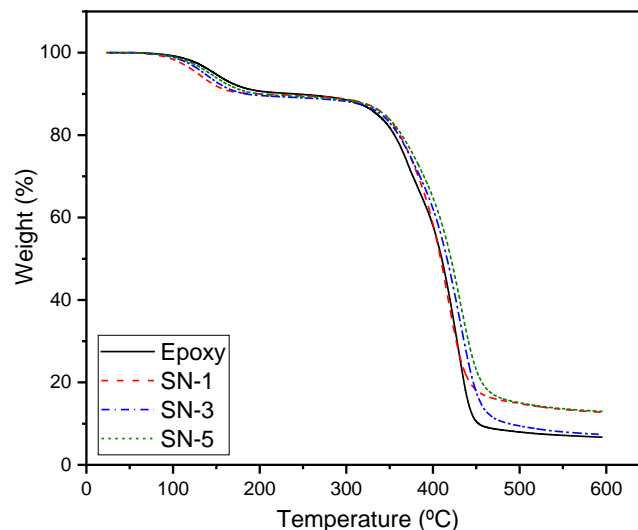
Figure 1. SEM images of (A) Epoxy, (B) SN-1, (C) SN-3, and (D) SN-5.

Table 2. Energy-dispersive X-ray spectroscopy (EDX) element detection and weight percentages.

Sample	Nanoparticle	Elements Present	Weight Percentage
Epoxy	–	C, O	78.94, 21.06
SN-1	SiO ₂	C, O, Si	78.33, 20.90, 0.77
SN-3	SiO ₂	C, O, Si	77.65, 20.80, 1.55
SN-5	SiO ₂	C, O, Si	76.24, 21.41, 2.34

3.2. Thermogravimetric Analysis (TGA)

Figure 2 shows the thermal behavior of the epoxy and SNP-modified epoxy coatings and Table 3 summarizes their degradation temperatures (Td). All of the curves depicted a similar weight loss pattern. A two-step degradation can be observed from the graphs. First, a step involves weight loss starting at approximately 100 °C, proceeding until approximately 300 °C, which involves the removal of solvent traces and other volatile substances, the degradation of residual reactants, or the decomposition of the resin's low molecular weight fractions [26–28]. Approximately 15% of the weight loss occurred in all of the formulations at this first stage of degradation.

**Figure 2.** Thermogravimetric analysis (TGA) curves of epoxy and silica nanoparticles modified epoxy coatings.**Table 3.** Degradation temperatures for unmodified and SiO₂ nanoparticle (SNP)-modified epoxy formulations.

Sample	Td, 15% ^a (°C)	Td, 25% ^b (°C)	Td, 50% ^c (°C)	Td, 75% ^d (°C)
Epoxy	335.74	367.26	410.20	431.78
SN-1	344.00	373.38	408.83	432.75
SN-3	340.42	373.48	416.31	440.75
SN-5	344.10	377.80	420.90	477.03

^a Temperature at 15% weight loss; ^b Temperature at 25% weight loss; ^c Temperature at 50% weight loss; ^d Temperature at 75% weight loss.

The second and major weight loss pattern started from 300 °C and continued to 500 °C. In this degradation profile, the decomposition percentages were recorded, as follows: epoxy (91%), SN-1 (83%), SN-3 (89%), and SN-5 (83%), respectively.

This major weight loss at the second stage of degradation above 300 °C is the result of the degradation of the epoxy resin [27,28]. With the addition of SNPs, an increase in thermal resistance is observed, as summarized in Table 3, where temperature at 15%, 25%, 50%, and 75% degradation

can be seen in increasing order. It can be clearly observed that the epoxy without nanoparticles at 15%, 25%, 50%, and 75% degradation withstands 335, 367, 410, and 431 °C, while the coating with 5% nanoparticles withstands 344, 377, 420, and 477 °C, which is significantly higher than the unmodified epoxy.

It is apparent from the results (Table 3) that the addition of nanoparticles increased the thermal stability of coatings, irrespective of the percentages added. The highest thermal stability was observed for the coatings with 5% SNPs. With an increasing silica content, the thermal stability of the epoxy SNPs increased. At higher temperatures, the SNPs move toward the surface because of silica's low surface potential energy. This silica acts as a thermal insulator and protects the polymer [29–31].

3.3. Mechanical Properties and Nanoindentation Test

The mechanical properties of coatings, such as impact strength and scratch resistance, were analyzed after complete curing (Table 4). An increase in both the impact and scratch resistance was observed in all of formulations, as compared with the epoxy without nanoparticles. With the addition of 5% SNPs, the impact strength increased from 64 to 128 lb/in² when compared to the epoxy without nanoparticles, while, in the case of scratch resistance, there is an increase from a 6 kg failure load for the epoxy to a 9 kg failure load with the addition of 5% nanoparticles.

Table 4. Mechanical properties of epoxy and silica modified epoxy coatings.

Sample	DFT (μm)	Pendulum Hardness	Impact (lb/in ²)	Scratch (kg)
Epoxy	70 ± 10	105	64	6
SN-1	70 ± 10	134	112	7
SN-3	70 ± 10	128	112	8.5
SN-5	70 ± 10	118	128	9

The epoxy imparts brittle behavior [32,33], and the increase in its mechanical properties is due to the contribution of the SNPs that increase the modulus [34,35]. This induced a plasticizing effect on the coatings, which, in turn, increased the scratch and impact properties.

Nanoindentation was performed on all of the coating formulations, attaining a maximum load of 100 mN, and typical load vs. displacement curves for all of the coating samples are shown in Figure 3. From the curves, it can be seen that no discontinuities are present (i.e. no significant jump in depth values), which suggests that no cracking occurred during the indenting phase. All of the formulations were subjected to similar loading conditions. From Figure 3, it can be seen that the incorporation of nanoparticles shifted the depth of all curves to lower values, which suggests that the incorporation increased the resistance of the coating against the indentation force; this, in turn, represents an increase in the load-bearing capacity of all the coatings. At the maximum load, the depth values for the epoxy formulation was 10,405 nm, with the addition of 1%, 3%, and 5% the maximum depth values were significantly reduced and restricted to 6360, 6249, and 6184 nm, respectively. This reduction of depth values suggests an increase in the hardness properties.

These load/depth curves were analyzed using software provided by Micro Materials to obtain the hardness and elastic modulus values. This analysis software used the Oliver and Pharr method [36] to derive the desired properties. The equations below show the parameters that were used to derive the hardness and modulus values:

$$HH = \frac{F_{max}}{A} \quad (1)$$

$$E_r = \frac{1 - \nu^2}{E} + \frac{1 - \nu_i^2}{E_i} \quad (2)$$

$$E = \frac{E_i E_r (1 - \nu^2)}{E_i - E_r (1 - \nu_i^2)} \quad (3)$$

where H is the hardness, F_{max} is the maximum load, A is the projected contact area at maximum load, E is the modulus of sample, ν is the Poisson's ratio (0.35 for polymer samples), E_r is the as reduced modulus, E_i (1141 GPa) is the modulus of diamond indenter, and ν_i (0.07) is the Poisson's ratio of diamond indenter [37–39].

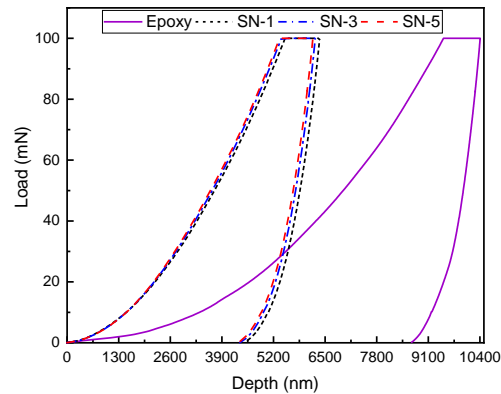


Figure 3. Load vs. depth curves of unmodified and SiO₂ modified coatings.

Figures 4 and 5 show the graphical representation of hardness and elastic modulus for all of the coating samples. Figure 4 shows an increase in hardness with the addition of nanoparticles from 0.08 GPa for the unmodified epoxy coating to 0.13 GPa for 1% addition, 0.14 GPa for 3% addition, and 0.15 GPa for 5% nanoparticle addition. Although an increase is observed in all of the added nanoparticle percentages, the highest hardness was obtained for the 5% formulation. Similarly, we can see that the modulus profile of all the coatings increased in all formulations from 3.04 GPa for the unmodified epoxy to 3.55, 3.67, and 3.73 GPa for 1%, 3%, and 5% formulations, respectively.

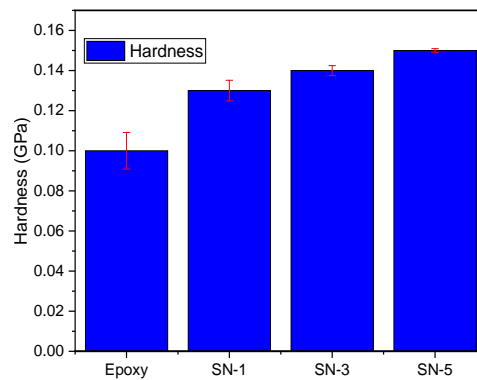


Figure 4. Indentation hardness of SNP formulated epoxy coatings.

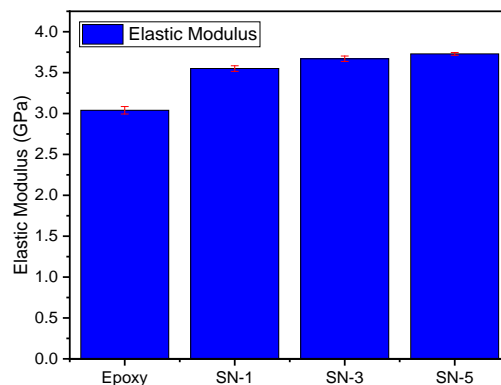


Figure 5. Indentation modulus of SNP formulated epoxy coatings.

The high modulus values of the modified coatings were due to the addition of the SNPs [40–42], which in turn, increased the modulus of the coatings [43]. The increase in hardness was mainly due to the free volume reduction in the cross-linked epoxy matrix. This reduction in the free volume happens due to the addition of nanoparticles [44,45].

3.4. Abrasion Resistance

The abrasion resistance (ASTM D4060) of silica incorporated coatings was determined using a taber abraser running 1000 cycles at each sample with the refacing of the wheels after 500 cycles. Refacing was performed for 50 cycles. The results that are shown in Figures 6 and 7 were obtained from the following equations:

$$\text{Mass Loss} = M_{\text{initial}} - M_{\text{damaged}}, \quad (4)$$

where M_{initial} represents the initial mass of intact coating (mg) and M_{damaged} represents the mass of the coating after abrasion (mg).

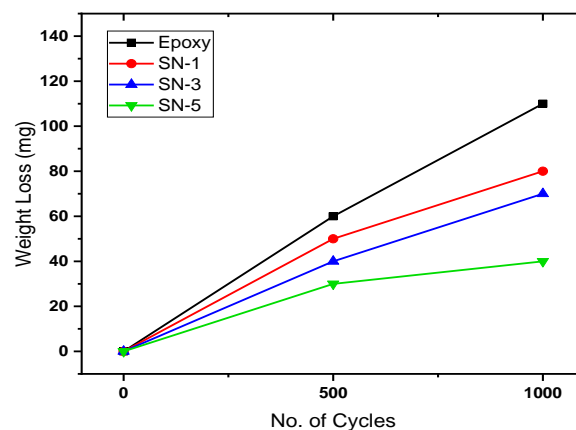


Figure 6. Weight loss for neat and modified epoxy coatings with different abrasion cycles.

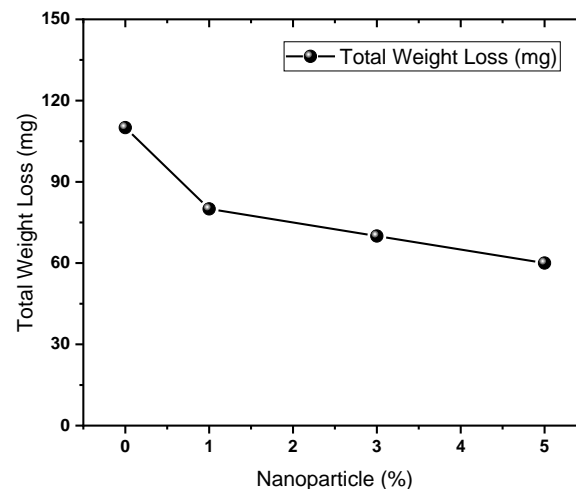


Figure 7. Mass loss with different nanoparticle percentages.

Figure 6 shows that the highest recorded weight loss was for the unmodified epoxy coating: 60 mg at 500 cycles and 110 mg at 1000 cycles. The addition of nanoparticles from 1% to 5% decreased the abrasion of the coatings, and the lowest abrasion was recorded with the 5% nanoparticles formulation. At 1000 cycles, a significant increase in the abrasion resistance was witnessed in comparison with the unmodified epoxy coating.

The results indicated an increase in the abrasion resistance with the addition of nanoparticles [7,46]. Figure 7 shows that the weight loss started to decrease with the addition of nanoparticles. The total

weight loss calculated was 60 mg with the addition of 5% SNPs, which was a 45% increase in the abrasion resistance when compared to the 110 mg weight loss of the epoxy without nanoparticles.

4. Conclusions

The effect of incorporation of SNPs on the mechanical, thermal, and abrasion properties of coatings using epoxy as a base matrix was evaluated. Morphological studies showed a good dispersion of the nanoparticles and some well distributed aggregates of the nanoparticles. The addition of the SNPs increased the overall mechanical properties; highest properties were obtained for the coatings with 5% SNPs. The coatings with 5% SNPs content showed approximately 50% improvements in the scratch resistance and 45% higher abrasion resistance when compared to the unmodified coatings. Nanoindentation results, such as hardness and elastic modulus were found to increase by 87% and 23%, respectively. Irrespective of mechanical properties, coatings with 5% SNPs resulted in better thermal properties and the decomposition temperature increased with an increasing content of the nanoparticles. These coatings provide excellent properties for application on various metal substrates and machinery parts where excellent mechanical properties are desirable.

Author Contributions: Conceptualization, M.A.A.; methodology, U.A.S.; formal analysis, M.A.A. and U.A.S.; writing—original draft preparation, U.A.S.; writing—review and editing, M.A.A., M.A. and A.A.; supervision, M.A.A., S.M.A.-Z.; project administration, S.M.A.-Z. and A.A. All authors have read and agreed to the published version of the manuscript.

Funding: This research and the APC was funded by the Research Supporting Project No. (RSP-2019/113), King Saud University, Riyadh, Saudi Arabia.

Acknowledgments: The authors would like to acknowledge the support provided by Research Supporting Project No. (RSP-2019/113), King Saud University, Riyadh, Saudi Arabia.

Conflicts of Interest: The authors declare no conflict of interest.

References

1. Sørensen, P.A.; Kiil, S.; Dam-Johansen, K.; Weinell, C.E. Anticorrosive coatings: A review. *J. Coatings Technol. Res.* **2009**, *6*, 135–176. [[CrossRef](#)]
2. Rong, M.Z.; Zhang, M.Q.; Liu, H.; Zeng, H.; Wetzel, B.; Friedrich, K. Microstructure and tribological behavior of polymeric nanocomposites. *Ind. Lubr. Tribol.* **2001**, *53*, 72–77. [[CrossRef](#)]
3. Ng, C.; Schadler, L.; Siegel, R. Synthesis and mechanical properties of TiO₂-epoxy nanocomposites. *Nanostructured Mater.* **1999**, *12*, 507–510. [[CrossRef](#)]
4. Ng, C.B.; Ash, B.J.; Schadler, L.S.; Siegel, R.W. A study of the mechanical and permeability properties of nano- and micron-TiO₂ filled epoxy composites. *Adv. Compos. Lett.* **2001**, *10*, 101–111. [[CrossRef](#)]
5. Shi, X.; Nguyen, T.A.; Suo, Z.; Liu, Y.; Avci, R. Effect of nanoparticles on the anticorrosion and mechanical properties of epoxy coating. *Surf. Coat. Technol.* **2009**, *204*, 237–245. [[CrossRef](#)]
6. Conradi, M.; Kocijan, A.; Zorko, M.; Verpoest, I. Damage resistance and anticorrosion properties of nanosilica-filled epoxy-resin composite coatings. *Prog. Org. Coat.* **2015**, *80*, 20–26. [[CrossRef](#)]
7. Palraj, S.; Selvaraj, M.; Maruthan, K.; Rajagopal, G. Corrosion and wear resistance behavior of nano-silica epoxy composite coatings. *Prog. Org. Coat.* **2015**, *81*, 132–139. [[CrossRef](#)]
8. Nikje, M.; Khanmohammadi, M.; Garmarudi, A.; Haghshenas, M. Nanosilica reinforced epoxy floor coating composites: Preparation and thermophysical characterization. *Curr. Chem. Lett.* **2012**, *1*, 13–20.
9. Fu, S.; Feng, X.-Q.; Lauke, B.; Mai, Y.-W. Effects of particle size, particle/matrix interface adhesion and particle loading on mechanical properties of particulate-polymer composites. *Compos. Part B Eng.* **2008**, *39*, 933–961. [[CrossRef](#)]
10. Qiang, F.U.; Shen, J.; Wang, G. Influencing factors of toughening HDPE with calcium carbonate rigid particles. *Polym. Mater. Sci.* **1992**, 107–112.
11. Weiyang, Q.U.I.; Jiwen, Y.U.; Yun, C.; Xianhua, Q.I.U. Development of All Starch Thermoplastics. *Chin. Plast. Ind.* **1998**, 106–108.
12. Liu, H.; Wang, G.-T.; Mai, Y.-W.; Zeng, Y. On fracture toughness of nano-particle modified epoxy. *Compos. Part B Eng.* **2011**, *42*, 2170–2175. [[CrossRef](#)]

13. Ahmad, F.N.; Mariatti, M.; Palaniandy, S.; Azizli, K.A.M. Effect of particle shape of silica mineral on the properties of epoxy composites. *Compos. Sci. Technol.* **2008**, *68*, 346–353. [[CrossRef](#)]
14. Sun, S.; Li, C.; Zhang, L.; Du, H.; Burnell-Gray, J. Effects of surface modification of fumed silica on interfacial structures and mechanical properties of poly(vinyl chloride) composites. *Eur. Polym. J.* **2006**, *42*, 1643–1652. [[CrossRef](#)]
15. Uddin, M.F.; Sun, C. Strength of unidirectional glass/epoxy composite with silica nanoparticle-enhanced matrix. *Compos. Sci. Technol.* **2008**, *68*, 1637–1643. [[CrossRef](#)]
16. Jiao, J.; Sun, X.; Pinnavaia, T.J. Mesostructured silica for the reinforcement and toughening of rubbery and glassy epoxy polymers. *Polymers* **2009**, *50*, 983–989. [[CrossRef](#)]
17. Mahrholz, T.; Stängle, J.; Sinapius, M. Quantitation of the reinforcement effect of silica nanoparticles in epoxy resins used in liquid composite moulding processes. *Compos. Part A Appl. Sci. Manuf.* **2009**, *40*, 235–243. [[CrossRef](#)]
18. Chasiotis, I. *Effect of Nanoscale Fillers on the Local Mechanical Behavior of Polymer Nanocomposites*; Illinois University at Urbana Department of Aerospace Engineering: Urbana, IL, USA, 2009.
19. Ji, X.-L.; Jing, J.K.; Jiang, W.; Jiang, B.Z. Tensile modulus of polymer nanocomposites. *Polym. Eng. Sci.* **2002**, *42*, 983–993. [[CrossRef](#)]
20. Islam, M. The Effect of Nanoparticle Size and Percentage on Mechanical Properties of Silica-Epoxy Nanocomposites. Master Thesis, Philadelphia University, Philadelphia, PA, USA, 2013.
21. Zhang, Y.-C.; Zhang, D.; Wei, X.; Zhong, S.; Wang, J. Enhanced tribological properties of polymer composite coating containing graphene at room and elevated temperatures. *Coatings* **2018**, *8*, 91. [[CrossRef](#)]
22. Luo, L.; Ma, Q.; Wang, Q.; Ding, L.; Gong, Z.; Jiang, W. Study of a Nano-SiO₂ microsphere-modified basalt flake epoxy resin coating. *Coatings* **2019**, *9*, 154. [[CrossRef](#)]
23. Yuan, H.; Qi, F.; Zhao, N.; Wan, P.; Zhang, B.; Xiong, H.; Liao, B.; Ouyang, X. Graphene oxide decorated with titanium nanoparticles to reinforce the anti-corrosion performance of epoxy coating. *Coatings* **2020**, *10*, 129. [[CrossRef](#)]
24. Alam, M.A.; Samad, U.A.; Sherif, E.-S.M.; Poulouse, A.M.; Mohammed, J.A.; Alharthi, N.; Al-Zahrani, S.M. Influence of SiO₂ content and exposure periods on the anticorrosion behavior of epoxy nanocomposite coatings. *Coatings* **2020**, *10*, 118. [[CrossRef](#)]
25. Karnati, S.R.; Agbo, P.; Zhang, L. Applications of silica nanoparticles in glass/carbon fiber-reinforced epoxy nanocomposite. *Compos. Commun.* **2020**, *17*, 32–41. [[CrossRef](#)]
26. Shimpi, N.G.; Kakade, R.U.; Sonawane, S.S.; Mali, A.D.; Mishra, S. Influence of nano-inorganic particles on properties of epoxy nanocomposites. *Polym. Technol. Eng.* **2011**, *50*, 758–761. [[CrossRef](#)]
27. Rubab, Z.; Afzal, A.; Siddiqi, H.M.; Saeed, S. Preparation, characterization, and enhanced thermal and mechanical properties of epoxy-titania composites. *Sci. World J.* **2014**, *2014*, 1–7. [[CrossRef](#)]
28. Samad, U.A.; Alam, M.A.; Chafidz, A.; Al-Zahrani, S.M.; Alharthi, N.H. Enhancing mechanical properties of epoxy/polyaniline coating with addition of ZnO nanoparticles: Nanoindentation characterization. *Prog. Org. Coatings* **2018**, *119*, 109–115. [[CrossRef](#)]
29. Lionetto, F.; Mascia, L.; Frigione, M. Evolution of transient states and properties of an epoxy–silica hybrid cured at ambient temperature. *Eur. Polym. J.* **2013**, *49*, 1298–1313. [[CrossRef](#)]
30. Gao, M.; Wu, W.; Yan, Y. Thermal degradation and flame retardancy of epoxy resins containing intumescent flame retardant. *J. Therm. Anal. Calorim.* **2009**, *95*, 605–608. [[CrossRef](#)]
31. Arabli, V.; Aghili, A. The effect of silica nanoparticles, thermal stability, and modeling of the curing kinetics of epoxy/silica nanocomposite. *Adv. Compos. Mater.* **2014**, *24*, 1–17. [[CrossRef](#)]
32. Fiedler, B.; Hojo, M.; Ochiai, S.; Schulte, K.; Ando, M. Failure behavior of an epoxy matrix under different kinds of static loading. *Compos. Sci. Technol.* **2001**, *61*, 1615–1624. [[CrossRef](#)]
33. Turk, M.; Hamerton, I.; Ivanov, D. Ductility potential of brittle epoxies: Thermomechanical behaviour of plastically-deformed fully-cured composite resins. *Polym.* **2017**, *120*, 43–51. [[CrossRef](#)]
34. Zhang, H.; Tang, L.-C.; Zhang, Z.; Friedrich, K.; Sprenger, S. Fracture behaviours of in situ silica nanoparticle-filled epoxy at different temperatures. *Polymers* **2008**, *49*, 3816–3825. [[CrossRef](#)]
35. Gibson, R.F. A review of recent research on mechanics of multifunctional composite materials and structures. *Compos. Struct.* **2010**, *92*, 2793–2810. [[CrossRef](#)]
36. Oliver, W.; Pharr, G. An improved technique for determining hardness and elastic modulus using load and displacement sensing indentation experiments. *J. Mater. Res.* **1992**, *7*, 1564–1583. [[CrossRef](#)]

37. Shen, L.; Wang, L.; Liu, T.; He, C. Nanoindentation and morphological studies of epoxy nanocomposites. *Macromol. Mater. Eng.* **2006**, *291*, 1358–1366. [[CrossRef](#)]
38. Krumova, M.; Flores, A.; Calleja, F.B.; Fakirov, S. Elastic properties of oriented polymers, blends and reinforced composites using the microindentation technique. *Colloid Polym. Sci.* **2002**, *280*, 591–598.
39. Chafidz, A.; Latief, F.H.; Samad, U.A.; Ajbar, A.; Al-Masry, W. Nanoindentation creep, nano-impact, and thermal properties of multiwall carbon nanotubes-polypropylene nanocomposites prepared via melt blending. *Polym. Technol. Eng.* **2016**, *55*, 1373–1385. [[CrossRef](#)]
40. Bray, D.J.; Dittanet, P.; Guild, F.; Kinloch, A.J.; Masania, K.; Pearson, R.; Taylor, A.C. The modelling of the toughening of epoxy polymers via silica nanoparticles: The effects of volume fraction and particle size. *Polymers* **2013**, *54*, 7022–7032. [[CrossRef](#)]
41. Hsieh, T.; Kinloch, A.J.; Masania, K.; Taylor, A.C.; Sprenger, S. The mechanisms and mechanics of the toughening of epoxy polymers modified with silica nanoparticles. *Polymers* **2010**, *51*, 6284–6294. [[CrossRef](#)]
42. Tetard, L.; Passian, A.; Lynch, R.M.; Voy, B.H.; Shekhawat, G.; Dravid, V.; Thundat, T. Elastic phase response of silica nanoparticles buried in soft matter. *Appl. Phys. Lett.* **2008**, *93*, 133113. [[CrossRef](#)]
43. Sattari, M.; Naimi-Jamal, M.R.; Khavandi, A. Interphase evaluation and nano-mechanical responses of UHMWPE/SCF/nano-SiO₂ hybrid composites. *Polym. Test.* **2014**, *38*, 26–34. [[CrossRef](#)]
44. Karasinski, E.; Da Luz, M.; Lepienski, C.M.; Coelho, L.A.F. Nanostructured coating based on epoxy/metal oxides: Kinetic curing and mechanical properties. *Thermochim. Acta* **2013**, *569*, 167–176. [[CrossRef](#)]
45. Lizundia, E.; Serna, I.; Axpe, E.; Vilas, J.L. Free-volume effects on the thermomechanical performance of epoxy-SiO₂ nanocomposites. *J. Appl. Polym. Sci.* **2017**, *134*, 45216. [[CrossRef](#)]
46. Malaki, M.; Hashemzadeh, Y.; Tehrani, A.F. Abrasion resistance of acrylic polyurethane coatings reinforced by nano-silica. *Prog. Org. Coat.* **2018**, *125*, 507–515. [[CrossRef](#)]



© 2020 by the authors. Licensee MDPI, Basel, Switzerland. This article is an open access article distributed under the terms and conditions of the Creative Commons Attribution (CC BY) license (<http://creativecommons.org/licenses/by/4.0/>).